TIME-DOMAIN SIMULATION OF FLOATING PIER AND MULTIPLE-VESSEL INTERACTIONS BY A CHIMERA RANS METHOD

Hamn-Ching Chen*
*Department of Civil Engineering
Texas A & M University
College Station, TX 77843, USA
hcchen@civil.tamu.edu

Erick T. Huang**
**Naval Facilities Engineering Service Center
1100 23rd Ave.
Port Hueneme, CA 93043, USA
Huangt@nfesc.navy.mil

Keywords: *Ship berthing; floating pier; berthing force; RANS method; chimera grids*

ABSTRACT

This paper presents results of a berthing analysis and their significance to the design of berthing facilities in unique conditions where traditional methods may not apply. The analysis was conducted with a Reynolds-Averaged Navier-Stokes (RANS) simulation model coupled with a six-degree-of-freedom motion code. This hybrid model treats the pier, moored and docking ships, and harbor basin as a coupled system. The simulation used real design parameters of a conceptual floating pier in an extremely shallow basin to emphasize fluid effects. Results indicate that the flow induced by a large ship berthing in shallow water has crucial impacts on all aspects of a ship berth. This flow essentially dictates the berthing energy and hence the fender forces. Ship induced hydrodynamic forces could be several times of ship inertia. The flow induced by docking ship further complicates couplings between floating pier and ships at berth. Fluid influences should hence be accentuated in the design of coupling structures for floating piers. Traditional methods for berthing energy assessment should be used with extra care for berthing operations involving large ship and floating pier under shallow water conditions.

1 INTRODUCTION

Marine fenders are crucial to a ship berth. A proper fender design should effectively absorb or dissipate the kinetic energy carried by a docking ship and thus mitigate the impact force to a sustainable level. Fender design normally involves extensive trade-offs depending on the type, purpose, site, function, and operation concept of a berthing facility. Berthing energy is nevertheless the common factor any feasible approach must address. Standard fender design practice to date uses a nominal berthing energy specified in terms of the displacement, approach speed, and attitude of a docking ship. Corrections due to ambient water, other ship characteristics, and site-specific factors are included via decoupled coefficients. Unfortunately, a reliable correction factor for fluid influence, or the added mass coefficient, is difficult to determine. Field measurements, if exist, are site specific and often disputable. This should not be a surprise as the present design method overly simplifies the complex, heavily site dependent, transient flow associated with ship berthing to a single correction factor. Besides, the concept of added mass implies association with ship acceleration. Yet, this simulation clearly indicates that the fluid influences to fender forces should be attributed to fluid acceleration rather than ship acceleration. This result partly explains the wide spreading of field measurements in the existing literature. Little evidence was found in favor of extending field measurements for use at other sites as ship induced flows are indeed dictated by basin geometry and facility layouts.

Fender design at a floating pier is further complicated by the presence of pier motion. As pier motion adds complexity to fender design, fender design also affects pier dynamics. Ship

induced flow could influences fender design through ship, floating pier, and their couplings. Fender selection is therefore no longer separable form pier design. Added mass coefficient alone is unable to capture sufficient insights of this crucial water flow in support of a proper engineering trade-off. A more accurate berthing energy assessment probably requires detailed three-dimensional numerical simulation in time domain. In the present study, the RANS method of Chen and Chen [1] and Chen et al. [2-4] was further extended for time-domain simulation of ship berthing at a floating pier in shallow water basin.

2 NUMERICAL METHOD

A chimera RANS method had been employed by of Chen et al. [1-4] for time-domain simulation of transient flow induced by a berthing ship. In their approach, the transport equations for both the momentum and turbulence quantities are solved using the finite-analytic method of Chen, Patel, and Ju [5]. To solve for the pressure, the PISO/SIMPLER pressure-velocity coupling technique of Chen and Patel [6] and Chen and Korpus [7] is used. The governing equations are summarized in this section.

In order to provide accurate resolution of the transient turbulent flows induced by berthing ships, it is necessary to solve the Reynolds-Averaged Navier-Stokes equations for incompressible flow in curvilinear coordinates:

$$U^i_{,i} = 0 \tag{1}$$

$$\frac{\partial U^i}{\partial t} + U^j U^i_{,j} + \left(\overline{u^i u^j}\right)_{,j} + g^{ij} p_{,j} - \frac{1}{Re} g^{jk} U^i_{,jk} = 0 \tag{2}$$

where U^i and u^i represent the mean and fluctuating velocity components, and g^{ij} is conjugate metric tensor. t is time, p is pressure, and $Re = U_o L/n$ is the Reynolds number based on a characteristic length L, a reference velocity U_o, and the kinematic viscosity n. Equation (1) represents the continuity equation and equation (2) represents the mean momentum equation. The equations are written in tensor notation with the usual summation convention assumed. The subscripts, $_{,j}$ and $_{,jk}$, represent the covariant derivatives. In the present study, the two-layer turbulence model of Chen and Patel [8] is employed to provide closure for the Reynolds stress tensor $\overline{u^i u^j}$.

In the chimera RANS method, the solution domain is first decomposed into a number of computational blocks. The body-fitted numerical grids for the ship and the harbor fluid domain are generated separately with the ship grid blocks completely embedded in the harbor grid. The ship grids are allowed to move with respect to the harbor grid in arbitrary combinations of translational and rotational motions. The PEGSUS program (Suhs and Tramel [9]) is employed every time step to determine the interpolation information for linking grids. In order to predict the ship and fender coupling flows, the chimera RANS method has been combined with a six-degree-of-freedom motion program developed by Huang [10] for Compound Ocean Structure Motion Analysis (COSMA) to facilitate the prediction of ship motions and fender loads.

The COSMA program was developed originally for potential flow simulations with the structural responses represented by a lumped mass-spring model. In this model, the structure is divided into a finite number of rigid body elements. The size of elements is selected on the basis of the complexity of the structure and the level of analysis detail desired. Each element is further simplified to a point mass with proper inertia located at the 'node', which is usually the center of gravity of the element. Elements are then connected with massless elastic springs to form an idealized model of the physical structure. The motion is described at nodes in accordance with

Newton's second law of motion. Motions at other locations on the structure can be calculated from the associated nodes by rigid body motion relations. The equation of motion implemented in the COSMA program can be written in the following general form:

$$[M+a]\{\ddot{X}(t)\}+[b]\{\dot{X}(t)\}+[K+C]\{X(t)\}=\{f(t)\} \tag{3}$$

where [M] is the generalized inertia matrix, [a] is the hydrodynamic mass matrix, [b] is the hydrodynamic damping matrix, [K] is the hydrodynamic restoring force matrix, [C] is the restoring forces due to coupling members, {$X(t)$} is the generalized displacement vector, and {$f(t)$} is the generalized external excitation force vector.

The COSMA program is capable of predicting the ship motions under wind, current, and waves. It handles multiple floating bodies with the presence of connectors, mooring lines, thrusters, and fenders. For the berthing operations considered here, ships and pier can be treated as rigid bodies and the coupling members to be included are fenders and mooring lines. Therefore, the [C] matrix reduces to a diagonal matrix with the coefficients representing the fender stiffness k for three translational modes. The floating pier and moored ship are rest in equilibrium and only the berthing ship is subjected to tug thrust. Moreover, wave forces are neglected as the scene is essentially in a fully sheltered harbor. As noted in Huang [10], the time dependent hydrodynamic force coefficients [a] and [b] were transformed from their frequency domain counterparts defined by potential theory with fluid viscosity being ignored. The present approach, however, directly computes the hydrodynamic forces acting on pier and ships in time without introducing added mass and damping coefficient matrices.

The present method solves the unsteady Reynolds-Averaged Navier-Stokes equations at each grid node for the transient velocity and pressure fields induced by the berthing ships. Therefore, the hydrodynamic force vector {$F_h(t)$} can be readily obtained by a direct integration of the surface pressure and shear stresses over the wetted hulls of the floating structures. Since the hydrodynamic forces {F_h} includes both the added mass and damping forces, Equation (3) can be rearranged in a convenient form as follows:

$$[M]\{\ddot{X}(t)\}+[K+C]\{X(t)\}=\{F_h(t)\} \tag{4}$$

For ship induced flows, the chimera RANS method was employed first to calculate the transient flow field and the associated hydrodynamic forces {$F_h(t)$}. The COSMA program was then used to solve the displacement vector {$X(t)$} from Equation (4). Once the new ship position and the corresponding fender deflection are determined, the numerical grids can be updated by following the ship motion. The PEGSUS program of Suhs and Tramel [9] is then used to pass the updated information between coupled blocks as required for chimera RANS simulations to proceed. In this coupled process, the COSMA code was considerably more sensitive to the size of time increments than the RANS program. Fender stiffness essentially limits the time increment for the motion code. In order to stabilize motion responses, the COSMA code advanced with a reduced time increment between steps of flow simulations. A ratio of 1/20 in general gave a good result in the present study. Yet, this shows little impact to the overall computational efficiency, as the COSMA code requires only a negligible fraction of the CPU time used by the chimera RANS simulations. The size of time increment for motion code is in fact determined by the stiffness of coupling members and the strength of fluid forces.

3 SIMULATION SCENARIO

The U.S. Navy is developing a floating pier as a potential replacement for the aging berthing facilities in use. This innovative pier features a double deck layout on modular construction with pontoon floats. It gains remarkable economical incentives from its operational versatility and relocatability. A floating pier, however, presents much hydrodynamic nature of a ship. Their performance is influenced by the ambient water and nearby vessels. As hydrodynamic data and design experiences pertinent to floating piers are scarce, an extensive analysis was launched to explore factors that may be critical to conceptual design, structural integrity and operational efficiency. Relevant fluid activities that most concern pier designers are those induced by berthing ships, harbor oscillations, and earthquakes. This article addresses the berthing effect, in which the pier and other entities in scene are treated as an integrated system. Figure 1 is a fisheye view of the pier layouts with two moored ships and a docking ship approaches the pier under the assistance of a tug. Recently, Huang and Chen [11] and Chen and Huang [12] examined parallel and oblique berthing scenarios, respectively, for pier layouts involving only one moored ship on the port side of the pier. These studies indicate that the flow field in the narrow conduit enclosed by the ships, the pier, and the sea floor critically affects the ship behaviors, especially as the docking ship draws near the close vicinity of the pier. The water mass driven by the docking ship primarily goes under the pier and around the moored ship due to the extremely small clearance under keel. This flow pattern continues due to the established fluid momentum despite the water supply being cut off as the docking ship stops at the fenders. This leads to an intense pressure deficit in the conduit, which continues to suck both vessels into the pier for an extensive duration. A second moored ship was added between the pier and docking ship in the present study to investigate her impact to the flow pattern and thus the interactions among vessels.

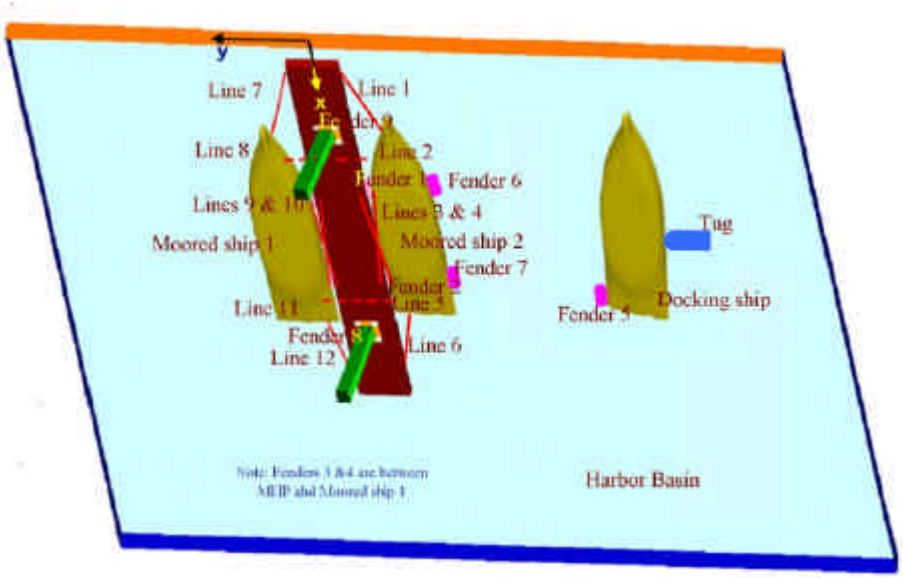

Fig. 1 – Ships and pier layout

Ship and Pier Particulars This conceptual pier shown in Figure 1 is a 1300 ft by 88 ft (396.25 m by 26.82 m) double deck floating pier constructed from identical 325-ft-long (99.06 m) modules. Two mooring dolphins are used to secure the pier, with their vertical shafts going through respect moon pools at roughly the quarter points of the hull. This unique mooring system along with internal fenders isolates the pier from earthquake effects and will hence reduce the premium for facilities built in earthquake areas. For the purpose of identifying the maximum

design loads imparted by docking ships, a worst-case scenario is selected as the test bed for the present simulation. Important particulars of the floating pier and vessels used in the simulation are summarized in Table 1. In addition, the characteristics of coupling members including fenders and mooring lines are listed in Table 2. For the purpose of identifying the fluid influence, all coupling members are simplified to linear springs.

	Pier	Ship
Displacement (tons)	42550	41150
Overall length (m)	396.25	237.14
Beam (m)	26.82	32.31
Draft (m)	4.36	8.23
Xcg from bow (m)	198.12	118.57
Ycg from centerline (m)	0	0
Zcg from waterline (m)	0	0

Table 1. Particulars of pier and vessels

Item	Characteristics
Foam fender (outer)	Diameter: 8 feet OD (2.44 m); Stiffness: 96 tons per meter
Trellex fender (inner)	Model: Trellex MX 1450; Stiffness = 806 tons per meter Maximum reaction: 307 tons
Mooring lines	Diameter: 3 inches (7.6 cm); Maximum tension: 13 tons

Table 2. Dynamic characteristics of coupling members

Layouts of simulation model The floating pier is extending from a vertical quay (in orange color), with a gap of 32.3 meters, into a wide-open harbor basin as shown in Figure 1. This sketch only shows the vicinity of floating pier. The actual fluid domain covers an area of 2,377 m wide by 2,463 m long. Details of numerical grid systems will be addressed in the section follows. The outboard end of the pier will be considered as the bow in this paper. A global reference is set at where the center plane of the pier intersects the quay wall at the elevation of free water surface. The x-axis extends along the pier length into the basin, while y-axis points to the port side and z-axis directs upward to complete a right hand coordinate system. The floating pier is secured with two dolphin shafts through moon pools at roughly the quarter points along the pier. These mooring shafts are surrounded by inner fenders (i.e., Fenders 8 and 9 in Figure 1) attached to the pier hull enclosing the moon pools. A most probable largest client ship is chosen as the model for this simulation. One model ship is moored to the port side and a second ship was moored to the starboard side. Each moored ship was restrained by six symbolic mooring lines, which represent important features of a typical ship mooring. Four foam fenders are hung on both sides of the pier at the water surface to facilitate coupling with vessels. Fender 5 is attached near the stern, on the starboard side, of the docking ship to prevent hard contact when the ship approaches obliquely to the pier. In addition, Fenders 6 and 7 are hung on the port side of the second moored ship to facilitate coupling with the docking ship. Designations of these coupling structures are assigned in Figure 1. A docking ship initially at 182.88 m (600 ft) from the pier (center to center) will berth at either 0° (parallel berthing) or 5° oblique angles to pier under tug assistance. The tug applies a constant thrust of 21.85 tons on the way after going through a linear startup ramp in the initial 100 seconds. The docking ship was released by the tug at a short distance from touching the fenders and since drifted on her own into the berth.

Numerical grid system A generic harbor basin of constant depth was selected for this simulation. A shallow water depth of 8.53 m was intentionally chosen to confine the under keel clearance of the docking and moored ships to roughly 0.3 m, or 3.7% of the ship draft. All three ships are of identical hull of 41,150 tons. This combination of a deep draft with a small under keel clearance gives a worst case berthing force for fender design consideration. In the chimera domain decomposition approach, the ships, pier, and harbor grids can be generated independently with arbitrary grid overlaps. Figure 2 shows the 13-block numerical grid used in the present study. The pier and ship grids are embedded in the harbor basin grid and are free to move with respect to the harbor grids in arbitrary combinations of translational and rotational motions. Furthermore, the ship grids were allowed to extend below the basin floor as shown in Figure 2(c) such that the grid distortions can be minimized in the narrow under keel region. A phantom grid was then used to remove the grid points outside the harbor basin as shown in Figure 2(d). This chimera grid system enables us to accommodate the relative motions among the pier, ships, and the harbor without adaptive generations of body-fitted numerical grids at each time step. The general procedures for information exchange among overlapping or embedded grid blocks were described by Chen et al. [1-4]. This model uses a total of slightly over 1.1 million grid points.

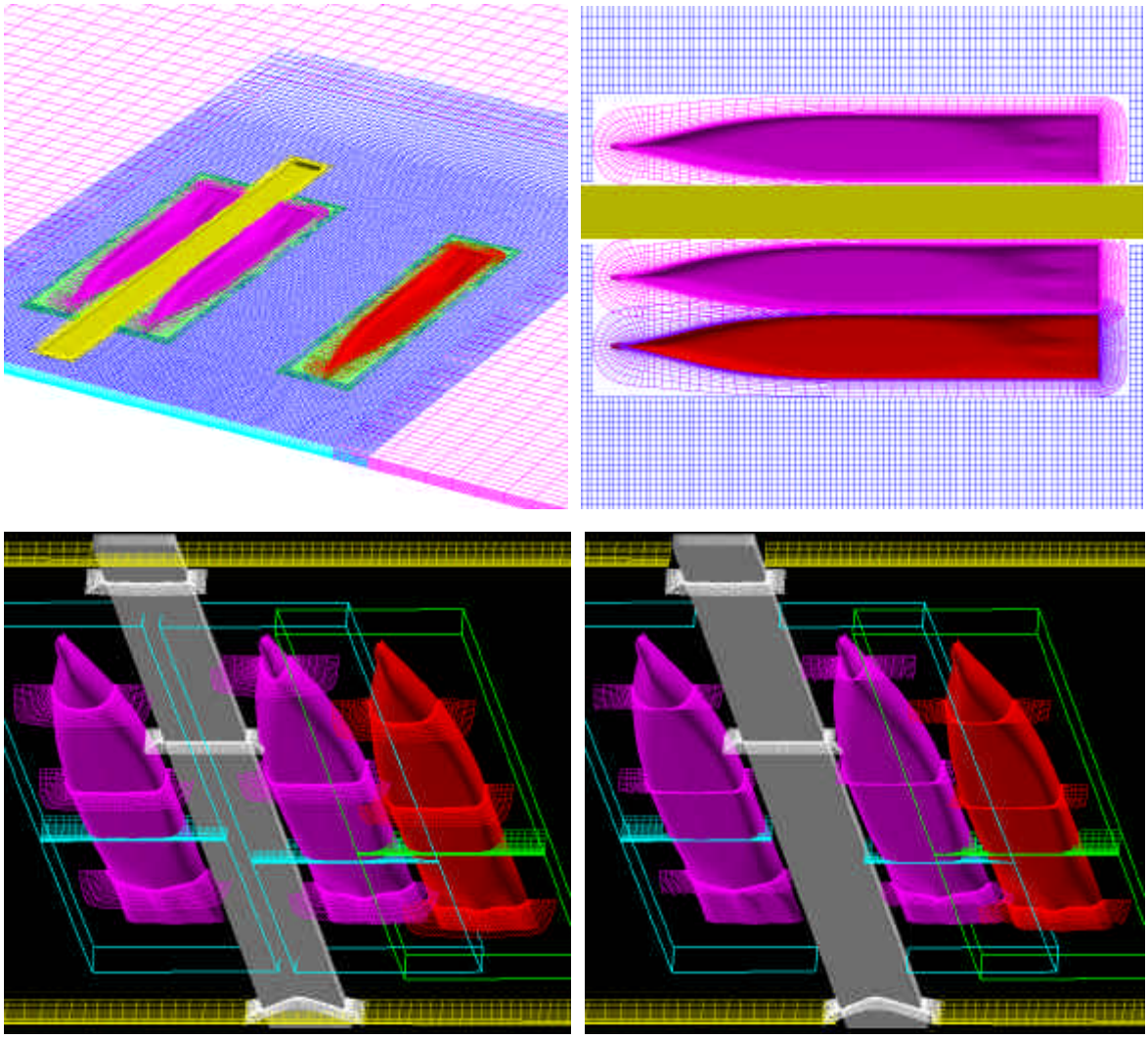

Fig. 2 – Solution domain and numerical grids

4 RESULTS AND DISCUSSION

The chimera grid system shown in Figure 2 was used to explore the impacts of ship berthing on pier dynamics. Simulations were performed with the docking ship approaching the pier parallel to or at an oblique angle of five degrees. For the sake of brevity, we will present detailed results for the 5° oblique berthing case only. Figures 3 and 4 show the computed pressure contours and velocity vectors at selected instants to illustrate the transient flow field induced by the docking ship and the interaction among the docking ship, moored ships, and the floating pier. For completeness, the force and motion histories of the docking ship, moored ships 1 and 2, floating pier, and coupling members (i.e., fenders and mooring lines) were also shown in Figures 5 thru 8 to facilitate a detailed analysis on the dynamic characteristics of the integrated pier system.

Docking Ship The docking ship started out with zero speed under tug assistance. The tug eventually applied a constant thrust of 21.85 long tons (Ltons) after going through an initial linear startup ramp of 100 seconds as shown in Figures 5(a) and 6(a). The docking ship continued to accelerate and gradually approaches a nearly constant speed of 0.19 m/s as seen in Figure 7(a) when the fluid resistance offset the tug thrust. It is further assumed that the tug was in full control and was able to maintain the docking ship at a 5° oblique angle to the pier before the tug thrust was shut off at t = 680 sec. It is seen from Figures 3 that the docking ship induced a strong pressure field in front and behind the ship path. The high-pressure ahead of the ship path propagates rather quickly toward the floating pier, subsequently bounces off the second moored ship, and returns to impact the docking ship. This has led to a pressure buildup between the docking ship and the second moored ship (Figures 3(d) – 3(i)), and a notable increase of fluid resistance on the docking ship (Figure 5(a)) prior to fender impact. Consequently, the docking ship oscillated slightly from early on and started to decelerate noticeably around 582 second time mark as seen in Figure 7(a), even though the tug still maintained the same thrust.

Upon released by the tug at a short distance away from the second moored ship, the docking ship was free to motions in water plane, namely surge, sway, and yaw, and continued to drift at a decreasing speed (Figure 7(a)) toward the pier under her own inertia until making fender contact with the second moored ship at t = 715 sec. It is seen from Figure 6(a) that the yaw angle of the docking ship increased to a maximum of 5.55° shortly after being released. The additional yaw in the counterclockwise direction can be attributed to the larger fluid resistance around the bow. As noted in Figure 4, the deep and narrow bow section produced much stronger flow recirculation and much higher resistance in comparison with the relatively flat and shallow stern section. This recirculation pattern persisted long after the docking ship stopped at the berth.

It is seen from Figure 8(a) that Fender 5 touched the second moored ship first because of the oblique approach of the docking ship towards the floating pier. The maximum fender compression force is about 44.5 Ltons during the initial impact. After the initial contact with pier, the docking ship begins to yaw clockwise as seen in the motion histories shown in Figure 6(a). It is interesting to note in Figure 8(a) that the docking ship decelerated the most rapidly, although very briefly, at the onset of fender compression when the fender reaction is low. This is mainly caused by the slight delay of the trailing water in response to ship deceleration. The trailing water caught up in a few seconds and quickly surpassed ship inertia as the primary contributor to the fender reactions. A high pressure region was developed on the port side of the docking ship (behind the ship path) as seen in Figure 3(i) – 3(k) due to the impingement of the trailing water on the ship hull as the ship decelerated and eventually rebounded completely from the pier at t = 725 sec. Shortly after the first rebound, Fender 5 made a second contact with even higher fender compression force of 59.0 Ltons between t = 732 sec and t = 741 sec (see Figure 8(a)) since the trailing water continued to push the ship towards the pier. The fender reactions for the three-ship

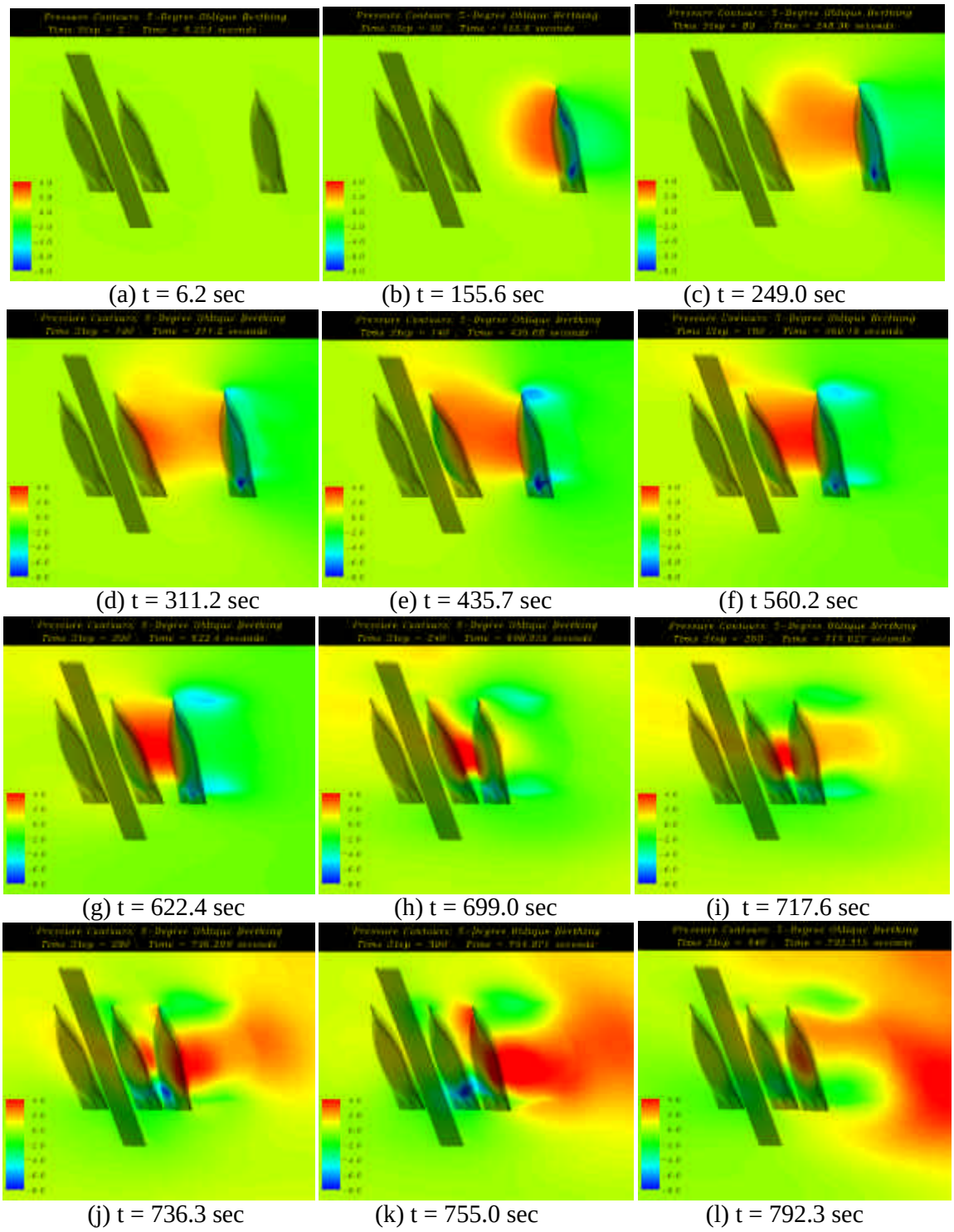

(a) t = 6.2 sec (b) t = 155.6 sec (c) t = 249.0 sec

(d) t = 311.2 sec (e) t = 435.7 sec (f) t 560.2 sec

(g) t = 622.4 sec (h) t = 699.0 sec (i) t = 717.6 sec

(j) t = 736.3 sec (k) t = 755.0 sec (l) t = 792.3 sec

Fig. 3 – Pressure contours around ships and pier

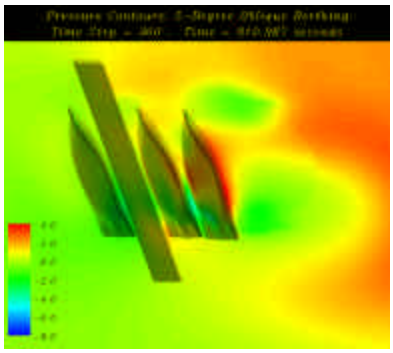

(m) t = 811.0 sec

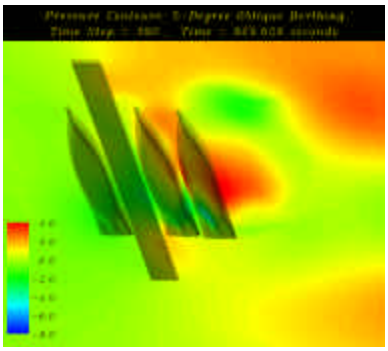

(n) t = 829.7 sec

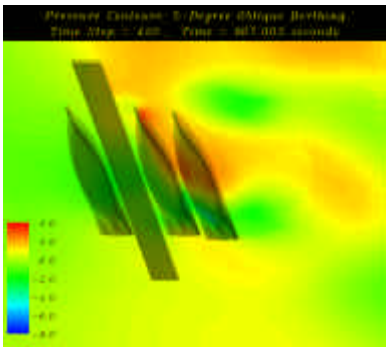

(o) t = 867.0 sec

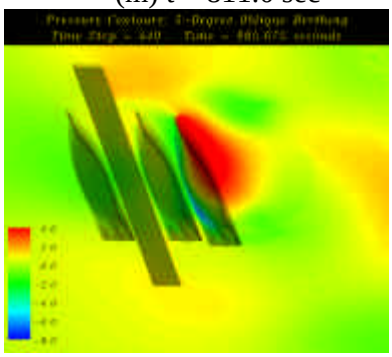

(p) t = 885.7 sec

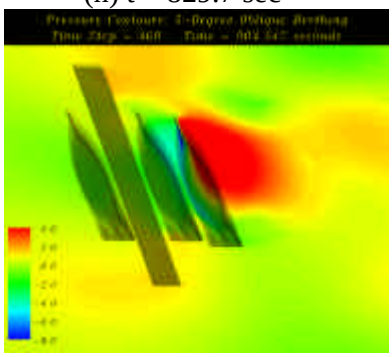

(q) t = 904.3 sec

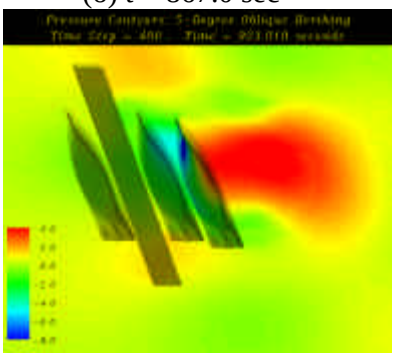

(r) = t = 923.0 sec

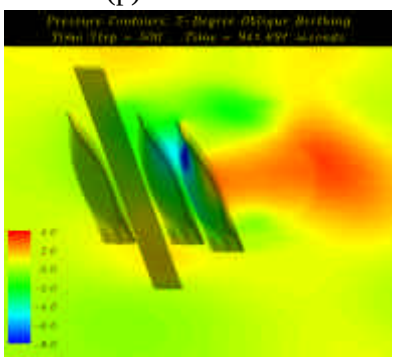

(s) t = 941.7 sec

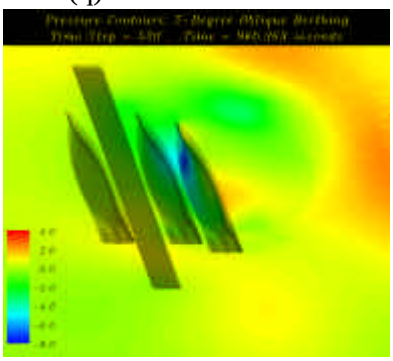

(t) t = 960.4 sec

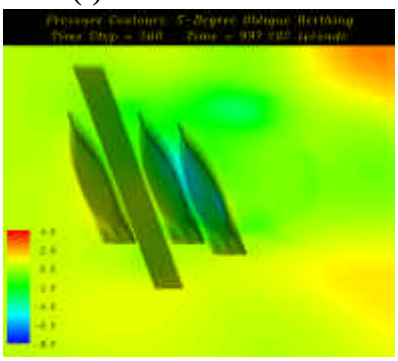

(u) t = 997.7 sec

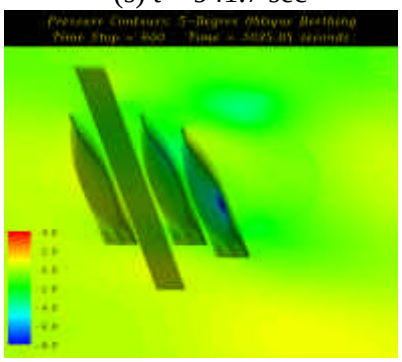

(v) t = 1035.1 sec

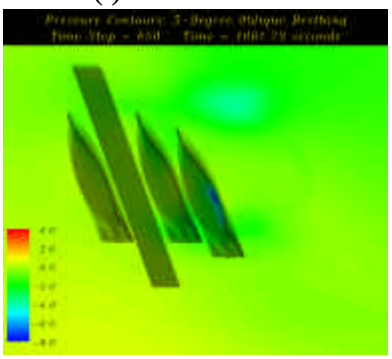

(w) t = 1081.73 sec

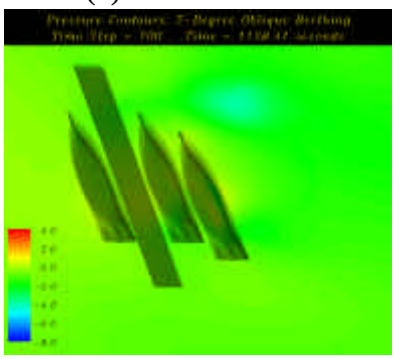

(x) t = 1128.41 sec

Fig. 3 – Continued

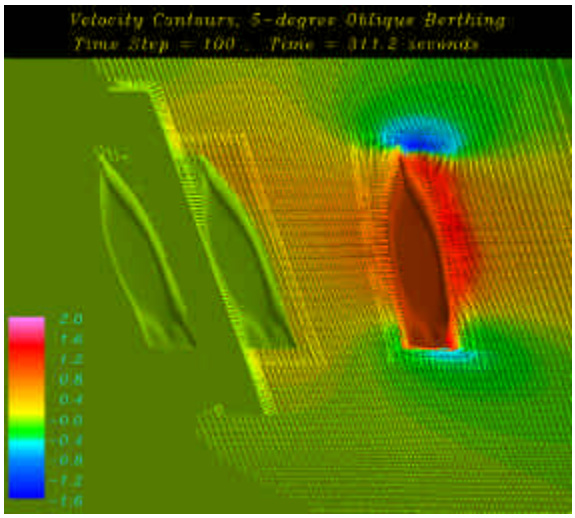

(a) t = 311.2 sec

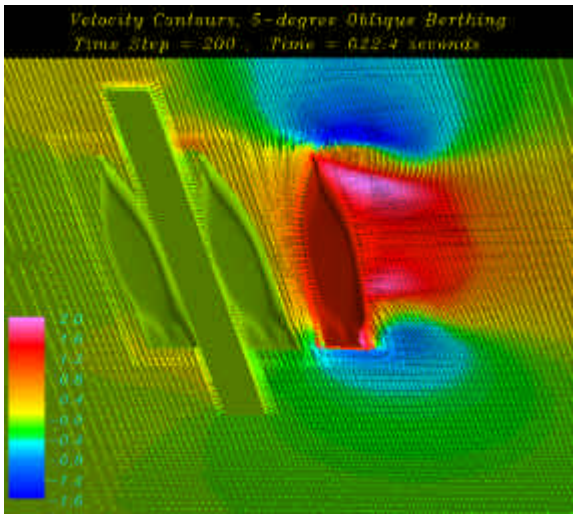

(b) t = 622.4 sec

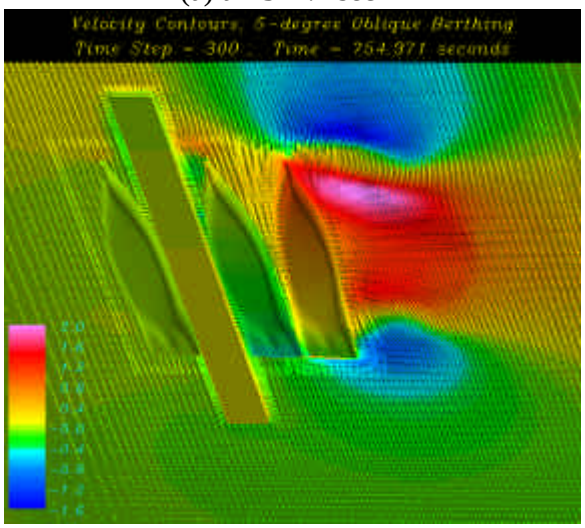

(c) t = 755.0 sec

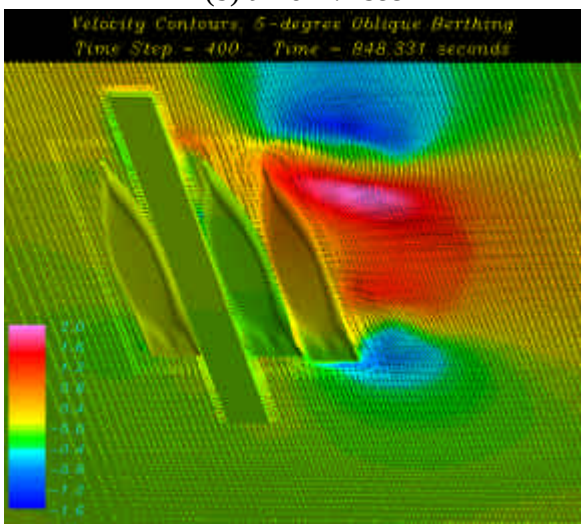

(d) t = 848.3 sec

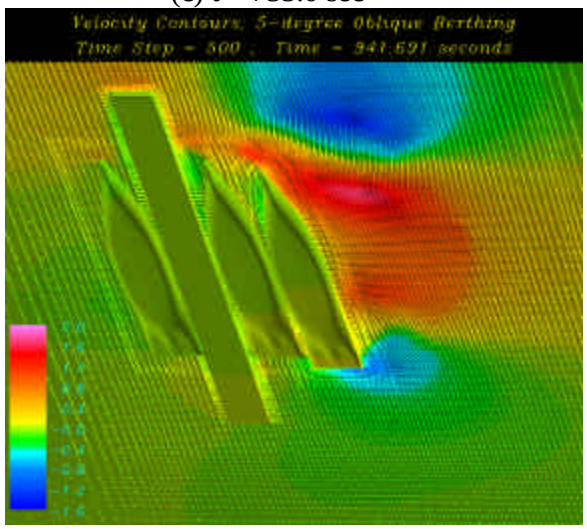

(e) t = 941.7 sec

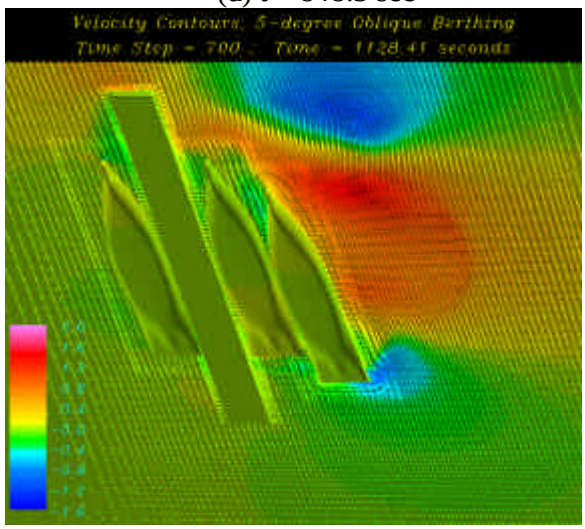

(f) t = 1128.4 sec

Fig. 4 – Velocity vector plots

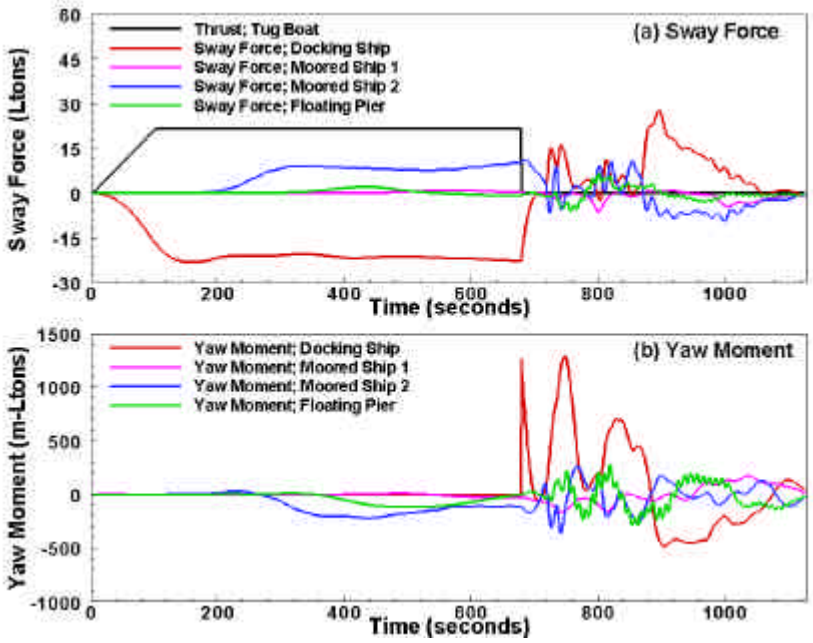

Fig. 5 – Sway forces and yaw moments acting on the ships and pier

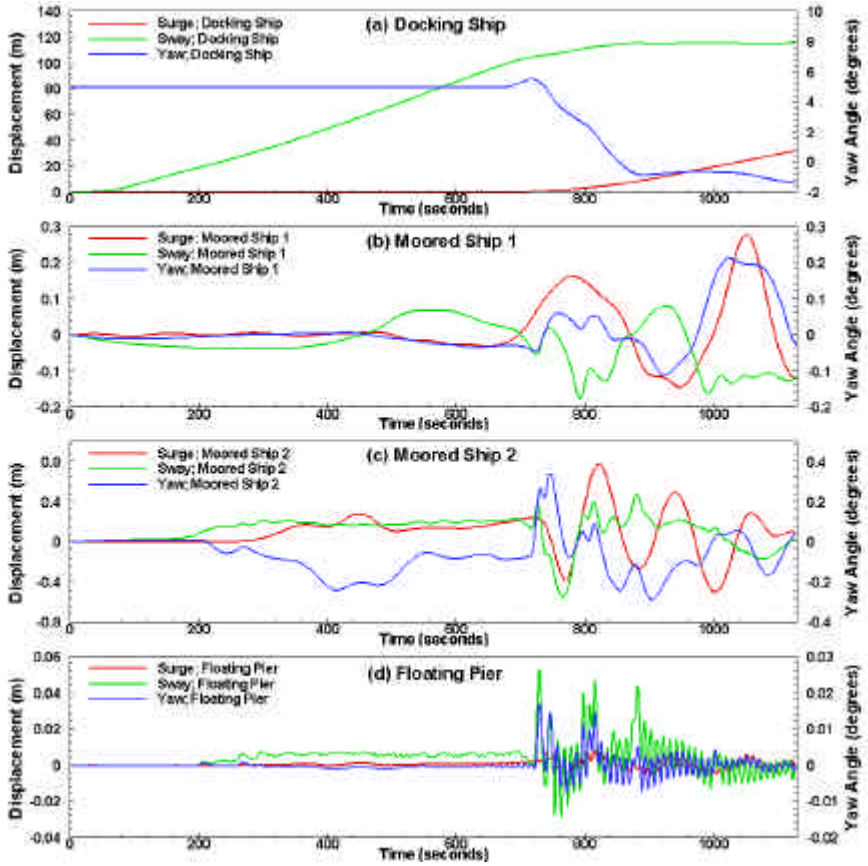

Fig. 6 – Motion histories of the ships and pier

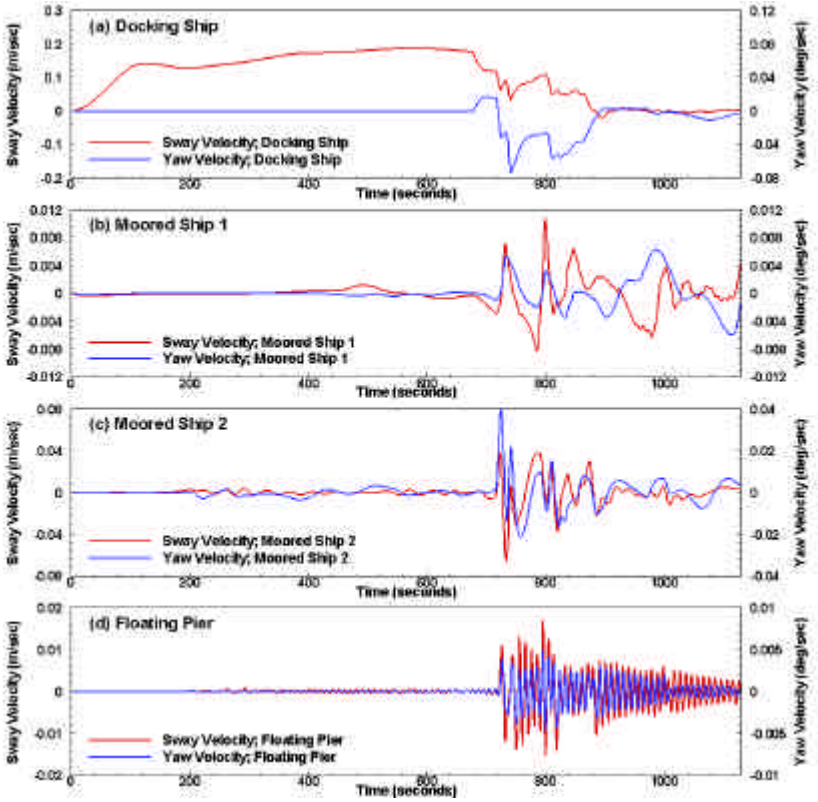

Fig. 7 – Sway and yaw velocities of the ships and pier

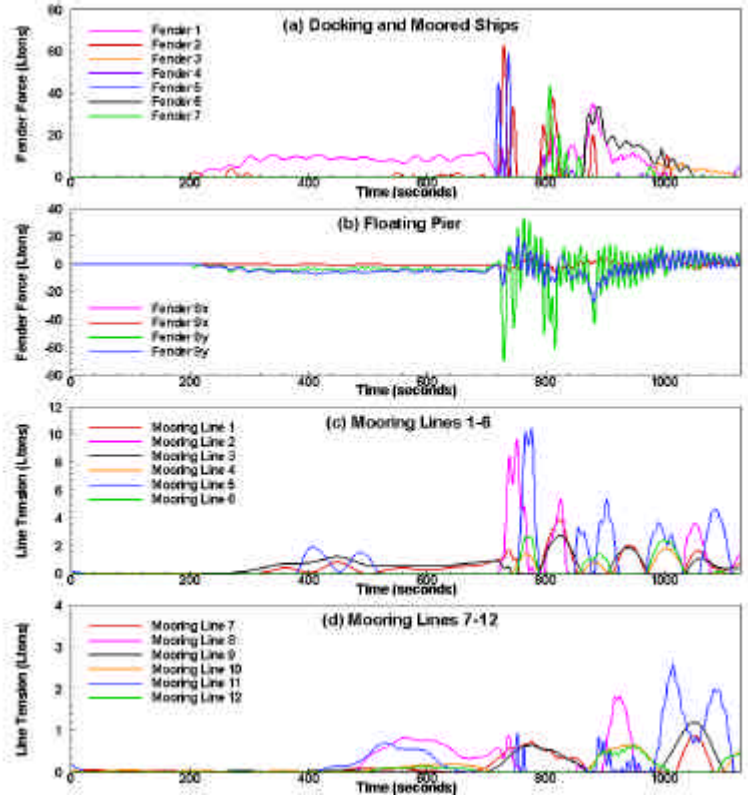

Fig. 8 – Fender forces and mooring line tensions

interaction case considered here is significantly more complicated than those observed in Chen and Huang [12] for the two-ship interaction case with the docking ship contacting the pier directly.

After the second rebound, the docking ship continued to yaw clockwise towards the pier as seen in Figures 3(j) – 3(n) and Figure 7(a). Due to the impact of the docking ship, the second moored ship was pushed towards the floating pier and made the primary impact with Fender 2 at t = 720 sec with a maximum fender force of 62.3 Ltons. The second moored ship rebounded from Fender 2 at t = 736 sec, but made another contact between t = 740 sec and 750 sec with a maximum loading of 33.1 Ltons. It is seen from Figure 8(a) that a large share of the berthing energy of the docking ship was absorbed during this stage with Fenders 5 and 2 took most of the impact loads. A detailed examination of Figure 8(a) indicates that the berthing energy was imparted first on Fender 5, and then transferred through the second moored ship to Fender 2 with several seconds of time delay. It is further noted from Figure 5 that a large yaw moment was developed around the docking ship at this stage with a rapid decrease of yaw velocity (Figure 7(a)) and a sudden slow down of the yaw motion as seen in Figure 6(a).

Due to the combined actions of the trailing water and the yaw motion, the docking ship made the primary impact with Fender 7 during t = 799 – 812 sec, followed by three additional impacts with smaller magnitude between t = 818 sec and t = 860 sec as seen in Figure 8(a). Shortly after rebounding completely from Fender 7, the docking ship made the primary contact with Fender 6 between t = 864 sec and t = 1049 sec. A large part of the berthing loads acting on Fender 6 was subsequently transferred through the second moored ship to Fender 1. It is seen from Figure 8(a) that stern fenders 2, 5 and 7 took most of the initial impact loads. However, the majority of the berthing energy was actually absorbed by the bow fenders 6 and 1 since they were in contact with the moored ship and floating pier for a much longer period of time.

The complete interaction among the docking ship, floating pier, moored ship, and fender systems produced a complex pressure system as shown in Figure 3. It is quite obvious that the transient flow induced by the vessel and pier motions (see Figures 3 and 4) plays a dominant role in determining the fender compression and maximum berthing loads. As noted in Huang and Chen [11], the ship inertia is not the primary contributor to the fender reactions except for a very brief period during initial fender compression. As soon as the trailing water caught up and fluid pressure developed, the pressure force overwhelmed ship inertia for the rest of berthing cycle. This pressure force is indeed hard to track to the ship acceleration at all. Ship inertia force is relatively small most of the berthing cycle.

Moored ships The moored ships and the floating pier began to experience pressure forces produced by the accelerating docking ship shortly after the latter took off as shown in Figures 5. Mooring lines clearly witnessed these forces from early on as seen in Figure 8. Tensions in mooring lines 7-12, which were used to restrain the motion of the first moored ship, increased as the docking ship approached the pier and relaxed rapidly after the docking ship hit the fenders. It is noted from Figure 8(d) that Lines 8 and 11 picked up most of the loads since they were used primarily to restrict the sway motion of the first moored ship away from the pier. It is worthwhile to note that the tensions on lines 7-12 are much smaller than those observed in Chen and Huang [12] in the absence of the second moored ship. This can be attributed to the sheltering effects of the second moored ship, which absorbed most of the berthing energy during fender impacts. Indeed, the sway and yaw motions of the second moored ship are two to three times of those encountered by the first moored ship as shown in Figure 6. Consequently, the maximum tensions on mooring lines 1-6 are also significantly higher than those experienced by lines 7-12 as shown in Figure 8. It is also noted that the tensions on Lines 2 and 5 are higher than the other mooring lines since they were used primarily to restrict the sway motion of the second moored ship.

After the docking ship hit the second moored ship at t = 715 sec, a strong pressure depression was developed in the narrow gap between the docking and moored ships as shown in Figures 3(j) – 3(k). As seen in Figure 6(c), the second moored ship was pulled towards the docking ship by the suction pressure forces after the initial fender impact. The tensions on Lines 2 and 5 increased sharply while the second moored ship was pulled away from the pier. It should be noted that the total forces acting on the second moored ship including fender forces from Fenders 1, 2, 5, 6, and 7, tensions from mooring lines 1-6, and hydrodynamic forces. The sway and yaw motions shown in Figure 6(c) were driven by the net forces and moments acting on the second moored ship. It is, therefore, essential to treat the floating pier, moored ships, docking ship, and coupling members (fenders and mooring lines) as an integral system in the analysis of the berthing loads.

Floating pier The floating pier is held by two stiff mooring dolphins and is free to heave otherwise. These dolphins are the ultimate anchors for the entire system. In addition to holding the floating pier from drifting, they also resist berthing loads transferring through outer fenders and secure ships at berth through mooring lines. Figures 7(d) and 8(d) summarize pier motion responses during berthing process. These dolphins are very effective in restricting the pier movement. The pier moved by no more than 0.10 m and rotated by less than 0.05 degrees in the berthing operation considered here. It reacted primarily to berthing forces and moments shown in Figure 5. Direct fluid force is too small to make meaningful impact. The pier surged at its nature frequency and was further modulated by the motion of the moored ships as seen in Figures 7. The pier deflected according to which of the two moored ships dominated. Since the motion of the second moored ship is significantly larger than that experienced by the first moored ship, the high frequency oscillation in sway mode of the floating pier was observed to be nearly in phase with the large displacements imposed by the second moored ships. The dynamic pressure throughout the berthing process was insignificant in comparison with the buoyancy force. Therefore, the pier is expected to float at its mean draft all the time. Its minor sway motion did not seem to affect the outer fenders either.

5 SUMMARY AND CONCLUSIONS

Time-domain simulation of ship berthing to a floating pier was simulated using a chimera RANS method coupled with a six-degree-of-freedom motion program. The floating pier, ships, and harbor basin are treated as an integrated system. This simulation used real design parameters in an extremely shallow water to illustrate the significance of fluid-induced forces to the facility design. The present RANS/COSMA method successfully captured many important features of the transient flow around the pier and ships at berth including the under keel flow acceleration, separation in the wake region behind the ship path, hydrodynamic couplings between the ships, floating pier, fenders, and mooring lines. All behaviors of vessels and coupling members can be clearly traced to the associated fluid activities. These insights allow fender and mooring system performance to be fully quantified to the details essential to hardware design. The simulation results clearly demonstrated that the transient flow induced by a large ship in very shallow water had crucial impacts on all aspects of a ship berth. This flow essentially dictates the berthing energy and hence the fender forces. Fluid influences should hence be accentuated in the design of coupling structures for floating piers.

6 REFERENCES

1. Chen, H.C. and Chen, M., "Chimera RANS Simulation of a Berthing DDG-51 Ship in Translational and Rotational Motions," *International Journal of Offshore and Polar Engineering*, Vol. 8, No. 3, pp. 182-191, 1998.
2. Chen, H.C., Chen, M. and Davis, D.A, "Numerical Simulation of Transient Flows Induced by a Berthing Ship," *International Journal of Offshore and Polar Engineering*, Vol. 7, No. 4, pp. 277-284, 1997.
3. Chen, H.C. and Huang, E.T., "Validation of a Chimera RANS Method for Transient Flows Induced by a Full-scale Berthing Ship," *Proceedings, 22nd Symposium on Naval Hydrodynamics*, Washington, D.C., August 9-14, 1998.
4. Chen, H.C., Liu, T., Huang, E.T., and Davis, D.A, "Chimera RANS Simulation of Ship and Fender Coupling for Berth Operations," *International Journal of Offshore and Polar Engineering*, Vol. 10, No. 2, pp. 112-122, 2000.
5. Chen, H.C., Patel, V.C. and Ju, S., "Solutions of Reynolds-Averaged Navier-Stokes Equations for Three-Dimensional Incompressible Flows," *Journal of Computational Physics*, Vol. 88, No. 2, pp. 305-336, 1990.
6. Chen, H.C. and Patel, V.C., "The Flow Around Wing-Body Junctions," *Proceedings, 4th Symposium on Numerical and Physical Aspects of Aerodynamic Flows*, Long Beach, CA, 16-19 January, 1989.
7. Chen, H.C. and Corpus, R., "A Multi-block Finite-Analytic Reynolds-Averaged Navier-Stokes Method for 3D Incompressible Flows," Individual Papers in Fluids Engineering, edited by F.M. White, ASME FED-Vol. 150, pp. 113-121, *Proceedings, ASME Fluids Engineering Conference*, Washington, DC, June 20-24, 1993.
8. Chen, H.C. and Patel, V.C., "Near-Wall Turbulence Models for Complex Flows Including Separation," *AIAA Journal*, Vol. 26, No. 6, pp. 641-648, 1988.
9. Suhs, N.E. and Tramel, RW, "PEGSUS 4.0 Users Manual," Arnold Eng Dev Center Rep AEDC-TR-91-8, Arnold Air Force Station, TN, 1991.
10. Huang, T.S., "Interaction of Ships with Berth at Floating Terminals," TM-65-90-03, Naval Civil Engineering Laboratory, Port Hueneme, California, 1990.
11. Huang, E.T. and Chen, H.C., "Ship Berthing at a Floating Pier," *Proceedings, 13th International Offshore and Polar Engineering Conference*, Vol. III, pp. 683-690, Honolulu, Hawaii, May 25-30, 2003.
12. Chen, H.C. and Huang, E.T., "Numerical Simulation of Dynamic Responses of a Floating Pier in Ship Berthing Operations" Paper No. EM-2003-136, *Proceedings, 16th ASCE Engineering Mechanics Conference*, University of Washington, Seattle, July 16-18, 2003.